# Research Article

Honggang Zhang, Weian Xuan, Jie Chen, Xiaolong Sun\*, and Yunchu Zhu

# Improving effect and mechanism on service performance of asphalt binder modified by PW polymer

https://doi.org/10.1515/rams-2024-0058 received March 31, 2024; accepted September 24, 2024

Abstract: To achieve the improving effect of polymer material on the sustainability of asphalt pavement materials, the PW modifier was selected as anti-aging modifier of asphalt. The microscopic morphology and structural characteristics of polymer modifier were characterized by using focused ion beam electron microscopy and energydispersive spectrometer. The functional group composition of the PW modifier was analyzed by Fourier transform infrared spectroscopy. The PW-modified asphalt was prepared for ultraviolet (UV) aging resistance evaluation. The microscopic morphology and surface roughness evolution of polymer-modified asphalt were investigated during the whole period of UV aging. Under the condition of UV aging, the functional group composition of polymer-modified asphalt was studied. The results showed that the microscopic morphology of the PW polymer modifier was mainly crystal structure, mainly composed of C and O elements. The PW polymer modifier could improve the aging resistance of asphalt binder effectively and alleviate the generation of asphalt microcracks in the process of UV aging. The addition of PW polymer modifier could inhibit the formation and accumulation of typical functional group inside asphalt binder during the UV aging period, which could achieve the effective control of asphalt UV aging behavior.

**Keywords:** pavement, asphalt, polymer, UV ageing, performance, mechanism

**Honggang Zhang, Weian Xuan, Jie Chen:** Guangxi Key Lab of Road Structure and Materials, Guangxi Transportation Science and Technology Group Co., Ltd, Nanning, 530029, China

Yunchu Zhu: School of Civil and Transportation Engineering, Guangdong University of Technology, Guangzhou, 510006, China

# 1 Introduction

To fulfill the driving comfort and road performance requirements, asphalt mixture is mostly selected as the main paving material in existing road engineering [1-3]. The asphalt pavement has sufficient viscoelasticity and appropriate strength, which has the advantages of good stability, smooth surface, and compactness [4,5]. However, long-term application of pavement would promote the failure of asphalt pavement, which is caused not only by unreasonable pavement structure and unsuitable asphalt materials but also by the coupling impact of light, heat, oxygen, water, and other external environmental factors [6-8]. Due to the repeated heating effect on asphalt mixture during mixing, paving, rolling and other construction processes, irreversible changes in technical performance would occur, namely, short-term aging of asphalt mixture [9,10]. Meanwhile, the coupling impact of light, heat, oxygen, water, and other external environmental factors would promote the aging of asphalt pavement material. After aging, the change of physical and mechanical properties of the asphalt mixture would leave failure hazards behind for subsequent application. These problems will accelerate the damage of asphalt mixture pavement and ultimately affect the service life of asphalt pavement [11-13].

The existing ultraviolet (UV) aging control solution of asphalt pavement materials is mainly achieved through the application of modifiers [14]. The commonly used UV aging modifiers mainly include UV absorbers, shielding agents, free radical trapping agents, and layered bimetallic hydroxides (LDHs). There are also differences in the mechanism, advantages, and disadvantages of different types of modifiers to achieve UV aging resistance of asphalt [15–18]. The UV absorber is one type of light stabilizer, which could absorb the UV part of sunlight and fluorescent light sources. After adding UV absorbent, this high-energy UV could be selectively absorbed to make it become harmless energy that could be released or consumed [19,20]. UV absorbers could be divided into the following categories according to their chemical structure: salicylates, phenylketones, benzotriazole,

<sup>\*</sup> Corresponding author: Xiaolong Sun, Key Laboratory of Road Structure & Material of Transport Ministry, Chang'an University, Xi'an 710064, China; School of Civil and Transportation Engineering, Guangdong University of Technology, Guangzhou, 510006, China, e-mail: xls1998@gdut.edu.cn

2 — Honggang Zhang et al. DE GRUYTER

substituted acrylonitrile, triazine, and others [21]. The shielding agent could shield the UV radiation and reduce the amount of UV radiation that finally reaches the asphalt surface for delaying the UV aging of asphalt [22,23]. The free radical trapping agent could capture the active free radicals generated by the molecular bond breaking in asphalt, and destroy the free radical chain reaction environment of photooxidation aging, which helps delay the UV light aging of asphalt [24-26]. The special structure of LDHs could endow them with the excellent functions of multilevel shielding, reflecting, and absorbing UV light, and could be artificially inserted into guest substances with specific functions. After being added into asphalt as a modifier, it could effectively delay the UV aging process of asphalt [27-29]. Although the existing modifiers could endow asphalt binder with anti-aging performance, there are also some application problems, such as compatibility problems and unstable application effect. Therefore, it is urgent to propose one type of modifier with good compatibility with asphalt and a stable application effect to effectively control the UV aging behavior of asphalt.

Based on this, PW polymer was selected as asphalt antiaging modifier. The microscopic morphology and structural characteristics of the polymer modifier were characterized by using focused ion beam electron microscopy (FIB-SEM) and energy-dispersive spectrometer (EDS). The functional group composition of the PW modifier was analyzed by Fourier transform infrared spectroscopy (FTIR). The PWmodified asphalt was prepared for UV aging resistance evaluation. The microscopic morphology and surface roughness evolution of polymer-modified asphalt were investigated during the whole period of UV aging. Under the condition of UV aging, the functional group composition of polymermodified asphalt was studied. This research will provide a relevant basis for the application of polymer modifiers in the control of the UV aging behavior of asphalt pavement materials.

# 2 Materials and methodology

# 2.1 Raw materials

# 2.1.1 Polymers

In this article, acrylonitrile styrene acrylate copolymer of UV resistance potential is selected as the asphalt modifier with the PW-957 (PW) model. The indicators of a PW polymer modifier are mainly presented in Table 1.

Table 1: Technical indices of PW polymer modifier

Technical indices	Testing value	Testing method
Proportion Ball indentation hardness (H 358/30)	1.07 g·cm <sup>−3</sup> 88.0 MPa	ASTM D792 ISO 2039-1
Vicat softening temperature	107°C	ISO 306/A120

#### 2.1.2 Asphalt

In this study, AH-70# asphalt was selected as the modification carrier of a PW polymer modifier, and the technical indices of AH-70# asphalt are mainly presented in Table 2.

# 2.2 Methods

# 2.2.1 Preparation of modified asphalt

AH-70# asphalt was placed in the heating oven of 120°C and heated for 6 h. Then a certain amount of molten asphalt was weighed and placed in a clean container, and the container was placed on the oil bath heating device at  $160^{\circ}$ C  $\pm$  5°C. A certain amount of PW modifier was weighed and added into the asphalt. The mixture was sheared and stirred for 30 min using the high-speed shear apparatus at the speed of 2,000 rpm. Before completion of preparation, PW-modified asphalt was subjected to insulation treatment and swelling. The preparation process of modified asphalt is shown in Figure 1.

# 2.2.2 Specimen preparation

## 2.2.2.1 Asphalt film preparation

The asphalt film is prepared by the stripping method for microscopic characterization, and the preparation process is shown as follows (Figure 2) [18]. A certain amount of

Table 2: Technical indices of AH-70# asphalt

Technical indices	Testing value	Testing method
Penetration	63.1 (0.1 mm)	T0604-2019
Ductility (10°C)	19.3 cm	T0605-2019
Ductility (15°C)	>100 cm	T0605-2019
Softening point	46.9°C	T0606-2019
Solubility (trichloroethylene)	99.5%	T0607-2019
Wax content	1.1%	T0615-2019

asphalt is poured into the culture dish for UV aging. The stripping solution (such as trichloroethylene and carbon disulfide) is placed in a new container. Then, the asphalt sample after UV aging is inverted in the container containing the solution. Asphalt with different aging layers could be obtained by dissolving at different times. After the solvent volatilizing completely, the asphalt in the container is dissolved into the film. The asphalt film thickness could be calculated according to the following formula:

$$F = \frac{M_{\text{film}}}{\pi(r)^2 \times \rho},$$

where F is the asphalt film thickness,  $M_{\text{film}}$  is the asphalt film weight, r is the asphalt film diameter, and  $\rho$  is the asphalt density.

# 2.2.2.2 Road performance specimen preparation

The preparation method of road performance test specimen is mainly performed referred to the Test Specification for Asphalt and Asphalt Mixture in Highway Engineering (JTG Correct E20-2019).

### 2.2.3 UV aging experiment

The UV weathering tester is used for UV aging treatment of asphalt test pieces. The intensity of UV aging irradiance is 1.2 W·m<sup>-2</sup>, and there are four irradiation tubes providing UV radiation. For the test specimens of road performance, only one side of the test specimen is subjected to UV aging irradiation to simulate the UV radiation condition of the upper surface pavement. For the microscopic characterization specimen, the upper surface of the asphalt film is irradiated by UV radiation. The UV irradiation time is 75, 150, 225, and 300 h.

#### 2.2.4 Performance test

#### 2.2.4.1 Physical property

Road performance test mainly includes the softening point test, ductility test, and penetration test. The road performance tests were performed following the Test Specification for Asphalt and Asphalt Mixture in Highway Engineering (JTG E20-2019).

# 2.2.4.2 Rheological property

The rheological performance test adopted the strain control mode with the controlled strain of 12% and the test frequency of 10 rad·s<sup>-1</sup>. The 25 mm parallel plates were selected, and the spacing was 1 mm. The experimental temperature ranged from 46 to 82°C, and the heating interval was 6°C. After reaching each set temperature, the test temperature was maintained for 10 min, and the shear composite modulus and phase angle values were recorded every 2 min. Five data points were obtained at each set temperature, and the average value was calculated.

#### 2.2.5 SEM-EDS test

The microscopic morphology characterization and composition analysis of polymer modifier and modified asphalt were carried out by using FIB-SEM and EDS. Before characterization, it is necessary to spray gold on the test piece with gold spraying equipment to increase its conductivity and stabilize the imaging quality. The magnification range of microscopic characterization is from 2,000 to 10,000 times.

# 2.2.6 Dynamic FTIR test

The chemical composition of the PW polymer modifier and modified asphalt was analyzed by thermogravimetry-infrared spectroscopy. The test was conducted in a nitrogen atmosphere.

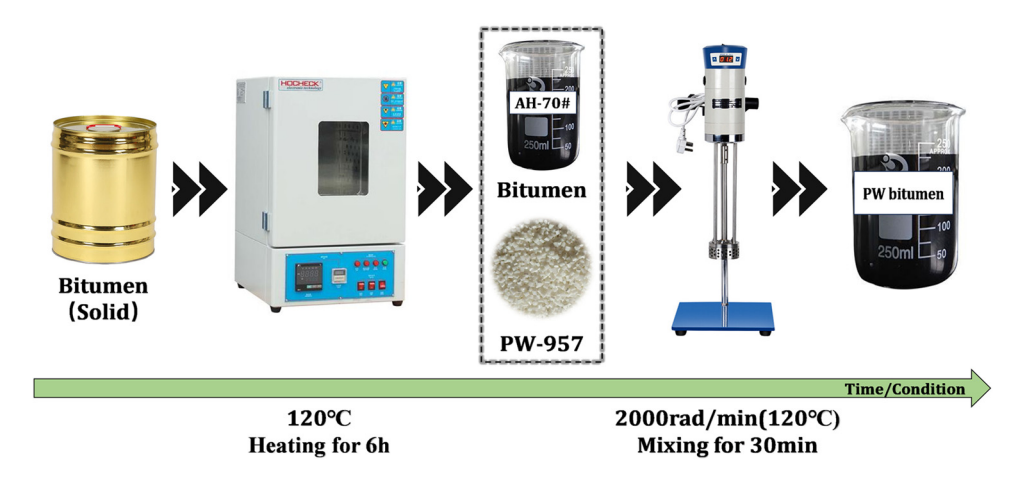


Figure 1: Preparation process of polymer-modified asphalt.

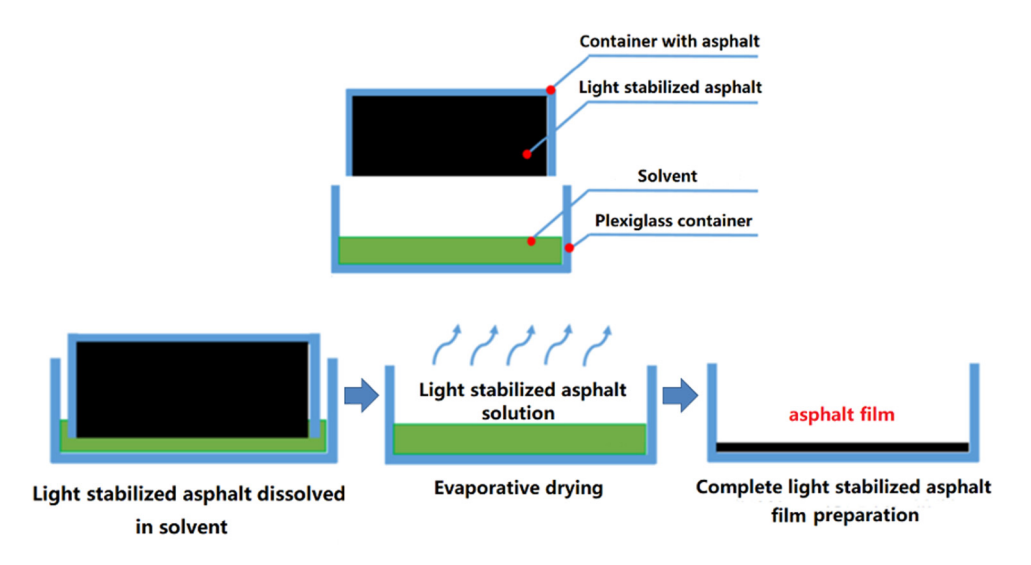


Figure 2: Preparation method of asphalt film [18].

#### 2.2.7 AFM test

The surface roughness of the asphalt specimen was characterized by Dimension FastScould AFM atomic force microscope. The characterization scale ranges from 30 to 80 µm (Figure 3).

# 3 Results and discussion

# 3.1 Microstructure and element composition of polymer modifier

# 3.1.1 Microstructure

Figure 4 shows the microscopic morphology characterization results of the PW modifier. It could be seen from the

analysis shown in Figure 4 that the microstructure of the PW modifier shows an obvious crystal structure. The particle surface is relatively smooth, and the particle shape is relatively regular. There are obvious edges and corners at the same time. After further magnification, it could be observed that the PW modifier surface has an obvious lamellar structure and presents a multilayer combination of microscopic morphology. According to the analysis of microscopic characterization results, the single-layer thickness range of the layered structure is about 0.3–1.2 μm. The particles of different modifiers are relatively independent, and there is no obvious agglomeration or contact. The particle size of the PW modifier is mainly distributed in the range of 5–26  $\mu$ m. The particle size of general particles is about 20 µM, basically consistent with the fineness of PW modifier 700 mesh. PW modifier has obvious edges and corners. At the same time, the lamellar structure

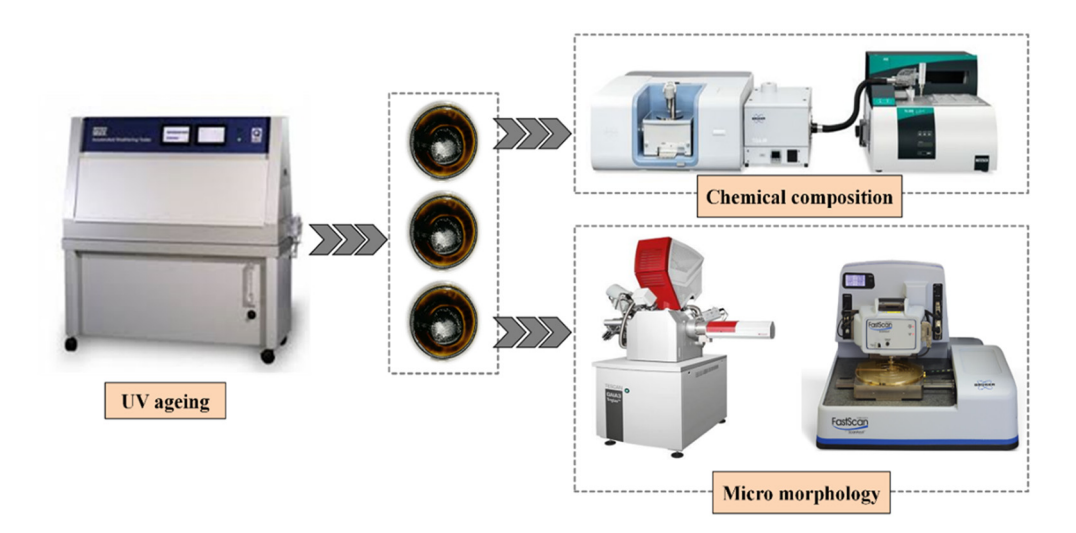


Figure 3: Testing plan of UV-aged polymer-modified asphalt.

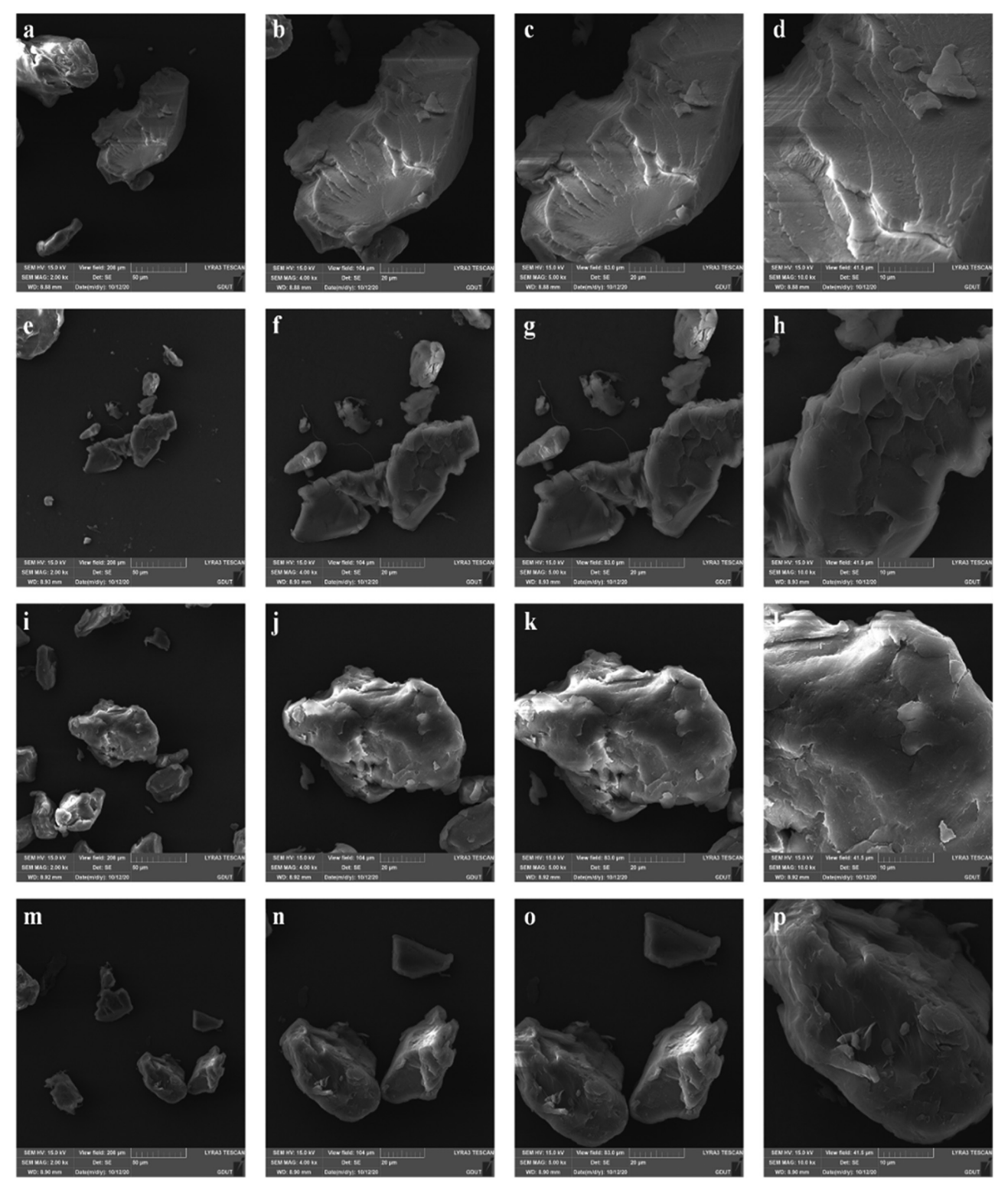


Figure 4: Micromorphology characterization results of polymer modifier. (a) view field1-2000 times, (b) view field1-4000 times, (c) view field1-5000 times, (d) view field1-10000 times, (e) view field2-2000 times, (f) view field2-4000 times, (g) view field2-5000 times, (h) view field2-10000 times, (i) view field3-2000 times, (j) view field3-4000 times, (k) view field3-5000 times, (l) view field3-10000 times, (m) view field4-2000 times, (n) view field4-4000 times, (o) view field4-5000 times, and (p) view field4-10000 times.

gives the particles a larger specific surface area, and the particles are relatively independent. Therefore, the PW modifier could form good adhesion and interaction with asphalt.

# 3.1.2 Element composition

The PW modifier particles in Figure 4(b) and (n) are selected as the main characterization objects for EDS analysis, and the results are shown in Figure 5. According to the analysis in Figure 5, the main components of the PW modifier are C and O, and their relative content could

reach more than 98%. At the same time, the chemical composition of the modifier also contains a small amount of H element, and the overall element composition is relatively simple. From the analysis of element mapping results (Figure 5(c), (d), (g), and (h)), we could see that the distribution range and the density of element C are relatively high. Combined with the results of the energy spectrum analysis of elements (Figure 5(i) and (j)), its content is obviously dominant, followed by the O element. EDS characterization results verified the purity and relatively simple element composition of the PW modifier. The pure element composition also promoted the fusion and interaction between asphalt and asphalt.

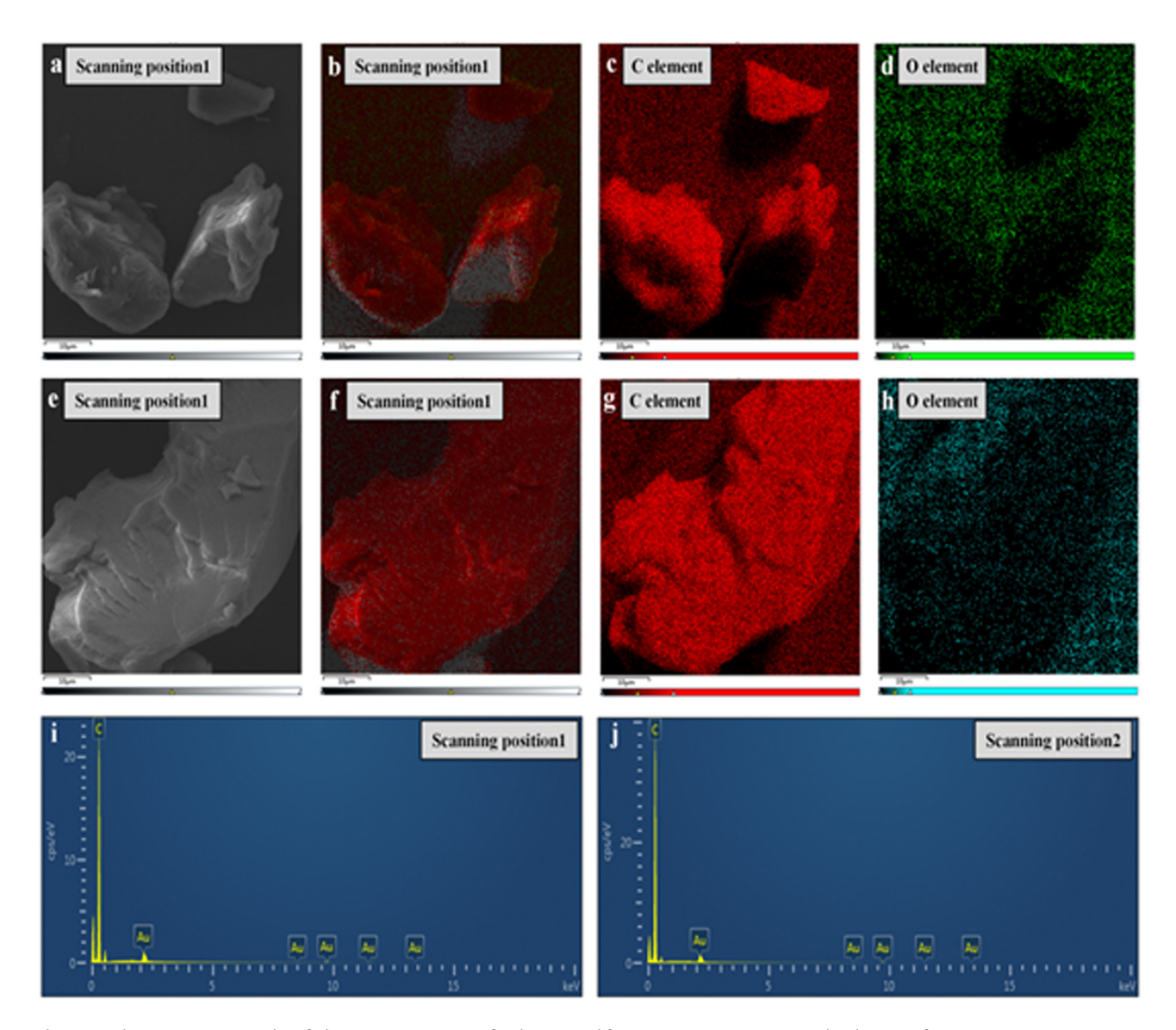


**Figure 5:** Characterization results of element composition of polymer modifier. (a) scanning position 1, (b) element of scanning position 1, (c) C element, (d) element, (e) scanning position 2, (f) element of scanning position 2, (g) C element, (h) element, (i) element composition of scanning position 1, and (j) element composition of scanning position 2.

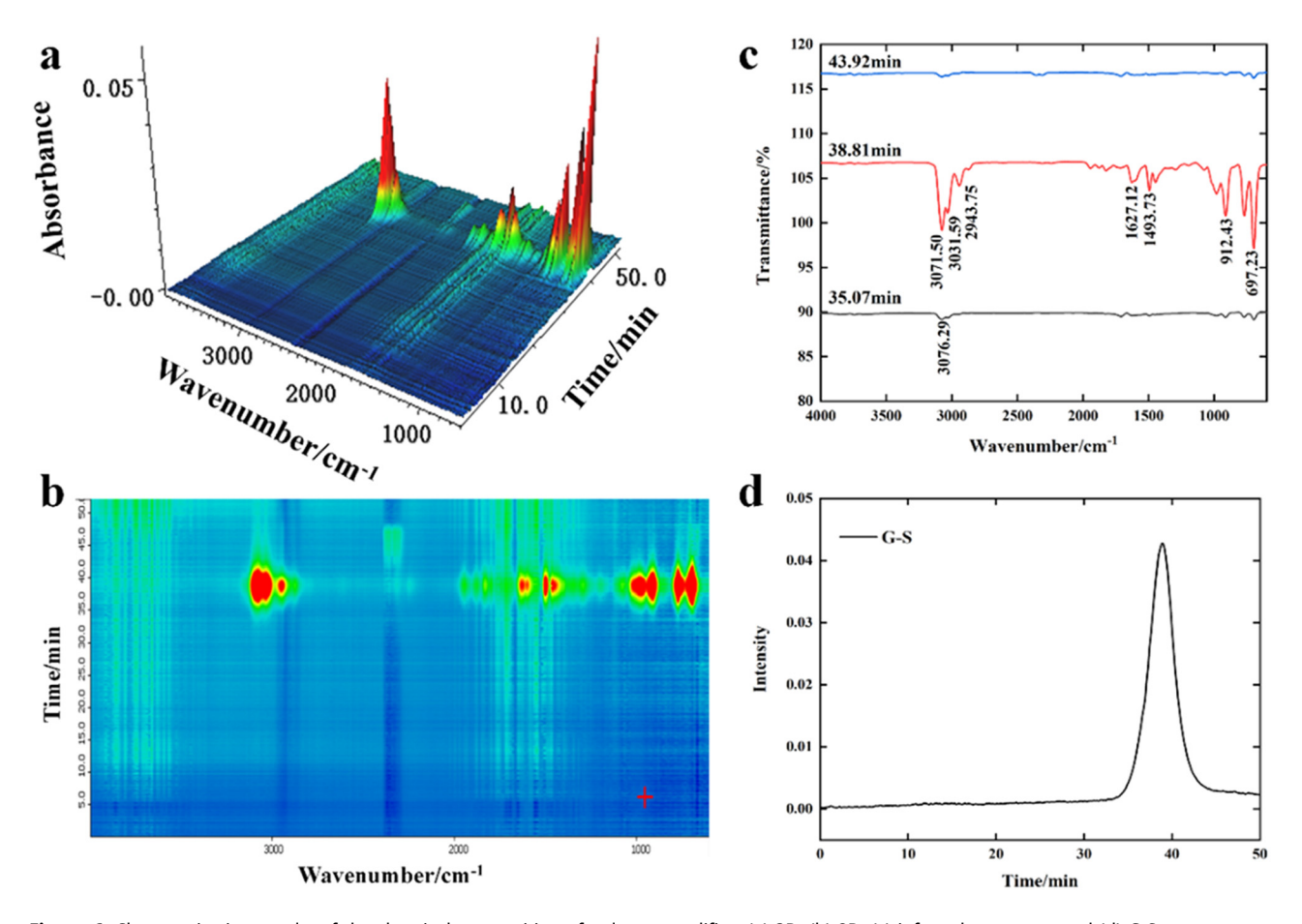


Figure 6: Characterization results of the chemical composition of polymer modifier. (a) 3D, (b) 2D, (c) infrared spectrum, and (d) G-S curve.

# 3.2 Chemical characters of polymer modifier

Figure 6 shows the dynamic FTIR characterization results of the PW modifier. The analysis in Figure 6 shows that the position of the characteristic peak of the PW modifier has hardly changed because of the difference in the intensity of the absorption peak caused by the change in temperature, which shows that the polymer decomposition is reflected in the amount of products at different temperatures during the heating treatment. It could be seen from the intensity curve that there was no material production in the first 35 min, and the weak peak of 3076.29 cm<sup>-1</sup> appeared only when the infrared spectrum curve was marked to 35.07 min. The intensity reaches the maximum value at 38 min. In the infrared spectrum, the accessory shoulder peak appears at 1493.73 cm<sup>-1</sup>, and the benzene ring stretching vibration appears at 1627.12 cm<sup>-1</sup>. The bending vibration of the aromatic ring occurs at 697.23 cm<sup>-1</sup>, while the characteristic peak at about 2,800 cm<sup>-1</sup> is the C-H symmetric stretching of -CH<sub>2</sub>-. With the increase of time, the intensity of each characteristic peak tends to be almost flat at 43 min. There is no obvious change in peak position and the appearance of new groups in the change of temperature.

# 3.3 Road performance of UV aged polymer-modified asphalt

# 3.3.1 Physical property

Figure 7 shows the pavement performance test results of base asphalt and PW-modified asphalt under different UV aging times. According to the analysis shown in Figure 7(a), with the extension of UV aging time, the softening point of base asphalt and PW-modified asphalt are significantly increased. This is mainly due to the increase of the content of heavy components in asphalt caused by UV aging, which significantly improves the viscosity of asphalt and thus increases the softening point of asphalt materials. At the same time, with the increase of the content of the PW modifier, the softening point also increased to a certain extent, but the increase rate was relatively small. According to the analysis shown in Figure 7(b), the ductility of asphalt decreases significantly with the increase of UV aging time. After aging for 300 h, the ductility is close to 0, and brittle fracture occurs during the test. This is mainly due to the volatilization of the light components in the asphalt after UV aging, the

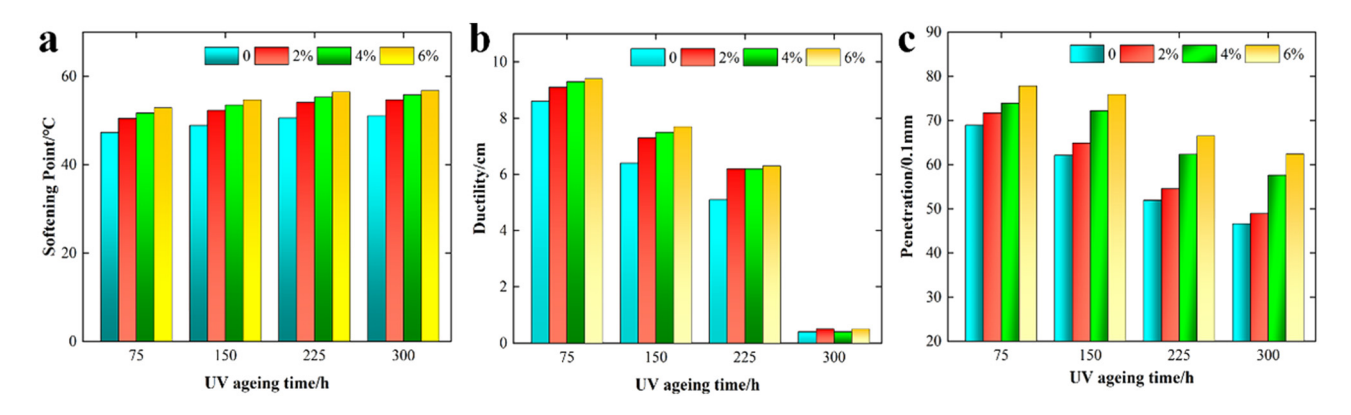


Figure 7: Test results of pavement performance of polymer-modified asphalt. (a) softening point, (b) ductility, and (c) penetration.

significant increase of the content of heavy components such as asphalt, which directly causes the asphalt to harden, and the obvious reduction of the deformability under low temperature, resulting in the low-temperature brittle fracture of the asphalt. In this process, PW modifier could significantly alleviate the decline of ductility caused by UV aging and could maintain the ductility of asphalt at a high level at the early and middle and late stages of aging, both higher than the ductility of base asphalt. However, the penetration test results are basically consistent with the ductility. The addition of the PW modifier improves the deformability of asphalt and could still maintain good deformability under the UV aging, so as to balance the high-temperature stability and low-temperature crack resistance. Based on this, the PW modifier has a good control effect on the UV aging of asphalt and could maintain the balance of various road performance of asphalt after UV aging, thus ensuring the stability of service performance.

#### 3.3.2 Rheological property

Figures 8 and 9 show the test results of the rheological properties of AH-70# asphalt and PW-modified asphalt.

From Figure 8, it could be seen that with the extension of UV aging time, the viscosity of AH-70# asphalt increased gradually, reflected as the complex shear modulus increasing gradually with UV aging time, while the phase angle decreased gradually. The rutting factor of the matrix asphalt increased with the extension of UV aging time, which indicated that the enhanced viscosity of the asphalt led to the hardening of the asphalt, and its resistance to load was enhanced. It could be analyzed from Figure 9 that the variation pattern of rheological performance indicators such as complex shear modulus and phase angle of PW-modified asphalt was basically the same as that of the base asphalt. This indicated that UV radiation still caused the generation and accumulation of UV aging characteristic groups inside the modified asphalt, gradually affecting the rheological properties of PW-modified asphalt.

According to the comparison of rutting factors between matrix asphalt and PW-modified asphalt in Figure 10, it could be known that the rutting factors of AH-70# asphalt and PW-modified asphalt showed the significant increasing trend with the extension of UV aging time. For the matrix asphalt, its rutting factor showed the stable increasing trend with the extension of UV aging time, indicating that the degree of aging of the matrix asphalt gradually increased with the extension of UV radiation time, reflected in the

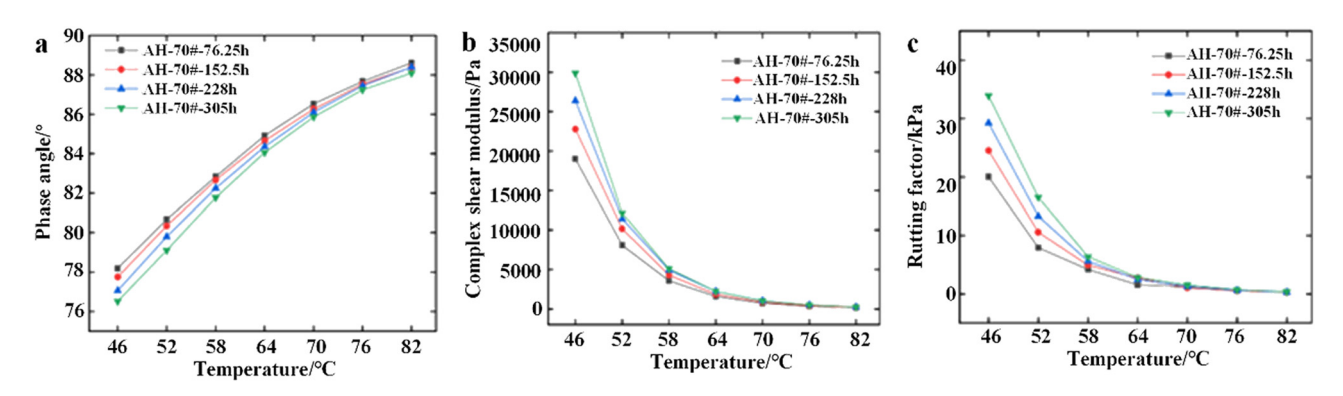


Figure 8: Test results of rheological property of AH-70# base asphalt. (a) phase angle, (b) complex shear modulus, and (c) rutting factor.

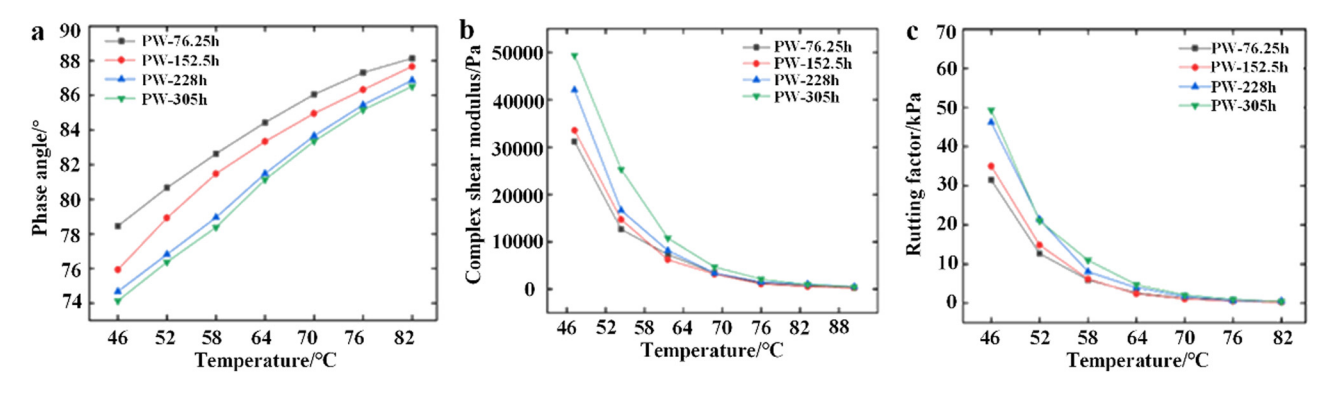
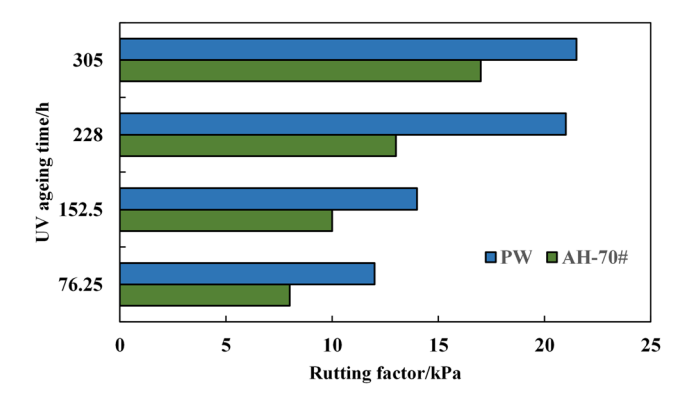


Figure 9: Test results of rheological property of PW modified asphalt. (a) phase angle, (b) complex shear modulus, and (c) rutting factor.



**Figure 10:** Comparison of rutting factor between PW-modified asphalt and AH-70# asphalt.

continuous and stable increase of the rutting factor in rheological properties. For PW-modified asphalt, during the early stage of UV aging (76.25–208 h UV irradiation), the rutting factor also showed the significant increase trend. However,

when the UV aging time continued to extend to 305 h, the rutting factor was basically similar to that of 208 h, which supposed that after certain amount of UV radiation time, the anti-UV aging performance of PW-modified asphalt gradually manifested, and the range of changes in its rheological properties gradually decreased. This also reflected that the PW modifier had the effective control effect on the UV aging behavior of asphalt binder.

# 3.4 Morphology variation of polymermodified asphalt following UV aging

# 3.4.1 Surface morphology

Figures 11 and 12 show the surface morphology and condition of the base asphalt and PW-modified asphalt film after UV aging at different times. Figure 11 shows that with the



**Figure 11:** UV aging surface condition of AH-70# base asphalt. (a) 1#-75h, (b) 1#-150h, (c) 1#-225h, (d) 1#-300h, (e) 2#-75h, (f) 1#-150h, (g) 2#-225h, (h) 2#-300h, (i) 3#-75h, (j) 3#-150h, (k) 3#-225h, (l) 3#-300h, and (m) 0h.



**Figure 12:** UV aging surface condition of polymer-modified asphalt. (a) 1#-75h, (b) 1#-150h, (c) 1#-225h, (d) 1#-300h, (e) 2#-75h, (f) 1#-150h, (g) 2#-225h, (h) 2#-300h, (i) 3#-75h, (j) 3#-150h, (k) 3#-225h, (l) 3#-300h, and (m) 0h.

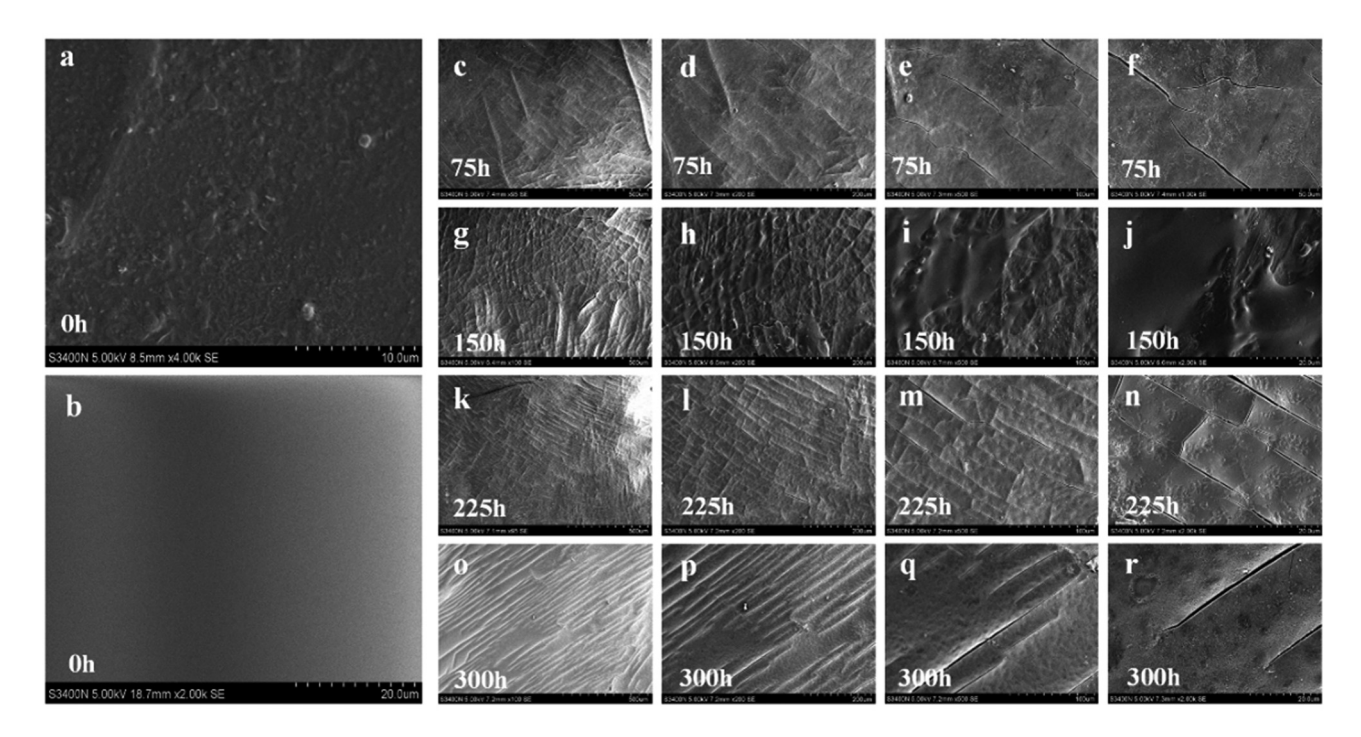


**Figure 13:** Ultraviolet aging microscopic morphology of AH-70# matrix asphalt. (a) 0h–4000x, (b) 0h–2000x, (c) 75h–100x, (d) 75h–200x, (e) 75h–500x, (f) 75h–1000x, (g) 150h–100x, (h) 150h–200x, (i) 150h–500x, (j) 150h–2000x, (k) 225h–100x, (l) 225h–200x, (m) 225h–500x, (n) 225h–2000x, (o) 300h–100x, (p) 300h–200x, (q) 300h–500x, and (r) 300h–2000x.

extension of the UV aging test piece, the surface condition of the base asphalt has changed significantly. When the UV aging time is 0 h, the surface of the asphalt film test piece is flat and smooth. At the same time, the volume of asphalt film is relatively regular, showing an obvious circular state. However, with the extension of the UV aging test piece, the asphalt test piece surface lost its original gloss. At

the same time, the surface flatness of the specimen decreased significantly, and obvious folds and cracks appeared. This is mainly due to the loss of light components in asphalt after UV aging, resulting in the reduction of asphalt deformability and then causing cracks and wrinkles in the process of volume change. At the same time, UV aging could also cause volume shrinkage of asphalt specimens.

Figure 12 shows that under the effect of UV aging, PW-modified asphalt surface also has obvious changes. When the UV aging time is 0 h, the surface of the asphalt test piece is smooth and shiny, and the surface is relatively flat. At the beginning of UV aging, PW-modified asphalt could still maintain good smoothness. However, with the further extension of UV aging time, PW-modified asphalt samples began to shrink to a certain extent, and the surface began to appear wrinkles and fine cracks. This is directly related to the volatilization of light components induced by UV aging. The surface condition of PW-modified asphalt after UV aging is similar to that of base asphalt.

## 3.4.2 Micro morphology

Figures 13 and 14 show the microscopic morphology characterization results of the matrix asphalt and PW-modified asphalt film specimens under UV aging conditions. The analysis in Figure 13 shows that the surface of the base asphalt without UV aging is smooth and flat, and there is no obvious fold or microcrack structure. When the UV aging time is extended to 75 h, obvious micro-cracks appear on the surface of the matrix asphalt specimen, and the cracks appear parallel. The cracks are relatively independent, and there are no longer through-type cracks. And there is

no obvious longitudinal connection between parallel cracks. When the UV aging time continues to extend to 150 h, the parallel independent cracks appear obvious longitudinal connection, and the cracks also gradually evolve from the original independent one-way cracks to the connected network cracks. Due to the obvious connection between cracks, the distribution density of cracks is significantly increased. But at the same time, in some micro-area, cracks also appear fusion and recovery, which may be due to the fracture healing caused by asphalt flow and fusion during UV aging. When the UV aging time is extended to 225 h, the cracks on the asphalt surface are still mainly through cracks. At the same time, the cracks have divided the asphalt surface into independent regular fragments, and the edges of the fragments also have some warpage. When the UV aging time is further extended to 300 h, the through-type cracks on the asphalt surface are healed and then restored to one-way parallel cracks. This is mainly because the asphalt has a certain degree of flow, thus achieving the healing and recovery of some cracks.

According to the analysis shown in Figure 14, with the extension of UV aging time, obvious cracks appear on the smooth PW-modified asphalt surface. When the UV aging time is 75 h, unlike the base asphalt, the cracks on the surface of PW-modified asphalt are more concentrated and closed, while the divided area is relatively smooth and

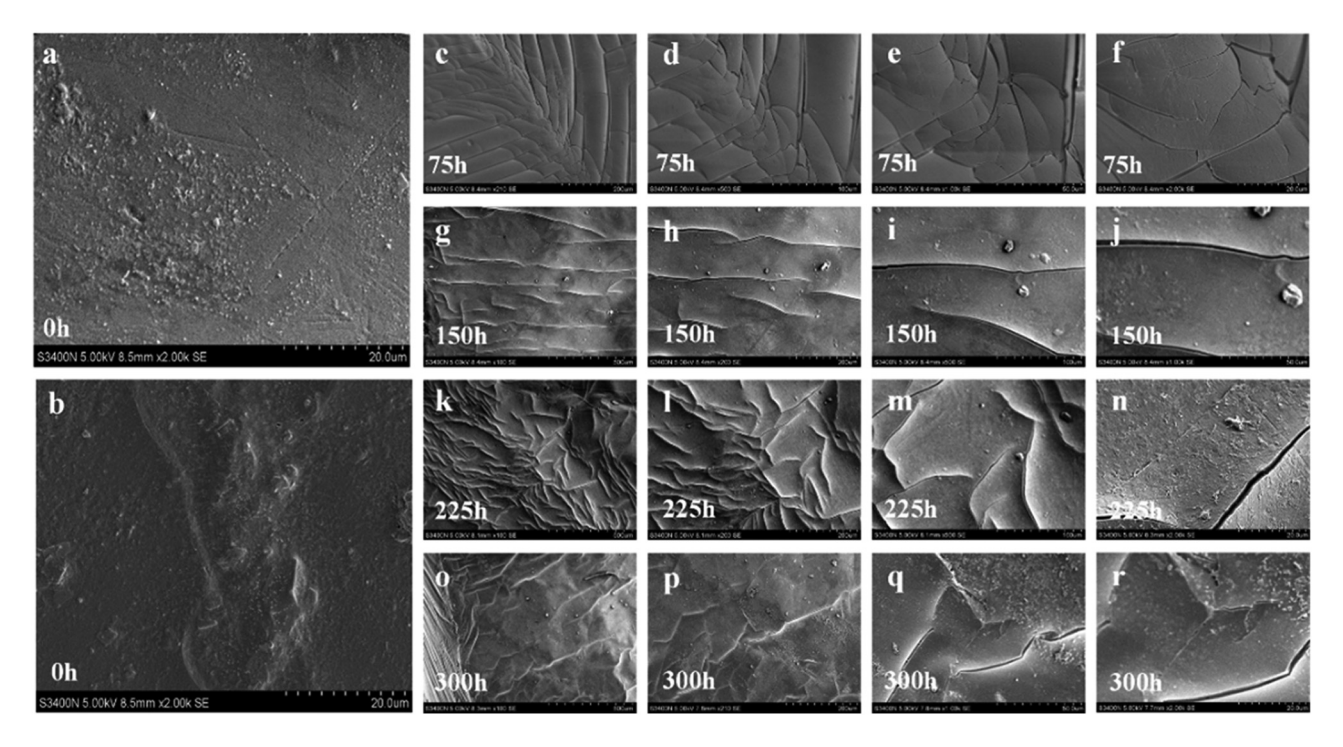


**Figure 14:** Ultraviolet aging microscopic morphology of polymer modified asphalt. (a) 0h–4000x, (b) 0h–2000x, (c) 75h–100x, (d) 75h–200x, (e) 75h–500x, (f) 75h–1000x, (g) 150h–100x, (h) 150h–200x, (j) 150h–2000x, (k) 225h–100x, (l) 225h–200x, (m) 225h–500x, (n) 225h–2000x, (o) 300h–100x, (p) 300h–200x, (q) 300h–500x, and (r) 300h–2000x.

flat. When the UV aging time reaches 150 h, the cracks change from aggregation to parallel independent cracks. There is no obvious connection and penetration between cracks, showing an obvious parallel state. At the same time, the width of the crack is also significantly widened. When the UV aging time is extended to 225 h, the cracks appear aggregated distribution again. The number of cracks per unit area is significantly increased, and the cracks are mostly unidirectional, and the directions are in different directions. When the UV aging time reaches 300 h, the number of cracks on the surface of the PW-modified asphalt specimen decreases significantly, and the width of cracks also decreases. This may be due to the flow and fusion of asphalt, resulting in the partial healing of cracks, thus reducing the number of cracks on the asphalt surface.

#### 3.4.3 Micro surface roughness

Figures 15–18 show the AFM characterization results of base asphalt and PW-modified asphalt. The analysis in Figures 15 and 16 shows that the surface roughness of nonaging matrix asphalt is relatively low, and the overall smoothness is good. With the extension of the UV aging test

piece, the surface roughness of the matrix asphalt test piece experienced an "increase – decrease – increase" trend. When the UV aging test piece reaches 75 h, compared with the nonaging test piece, the surface roughness of the matrix asphalt test piece is significantly increased, and a large number of local independent bulges appear, resulting in the fluctuation of the surface. When the UV aging time is extended to 150 h, the asphalt surface roughness will further increase, and some independent bumps will merge into larger bumps. When the UV aging time reaches 225 h, the roughness of the surface of the base asphalt is significantly reduced, and the number of independent bumps is reduced. which may be due to the flow and fusion of asphalt to a certain extent. When the UV aging time finally reaches 300 h, the roughness of the base asphalt surface increases slightly, but it is significantly lower than 75 and 150 h.

According to the analysis in Figures 17 and 18, the surface roughness of PW-modified asphalt is similar to that of base asphalt, but the surface condition at specific aging time points is different. The surface of the aged asphalt test piece is flat and smooth. However, with the extension of the UV aging time, the asphalt surface gradually appears as a large area of independent bulges, and the roughness is significantly improved. When the UV aging time reaches 75

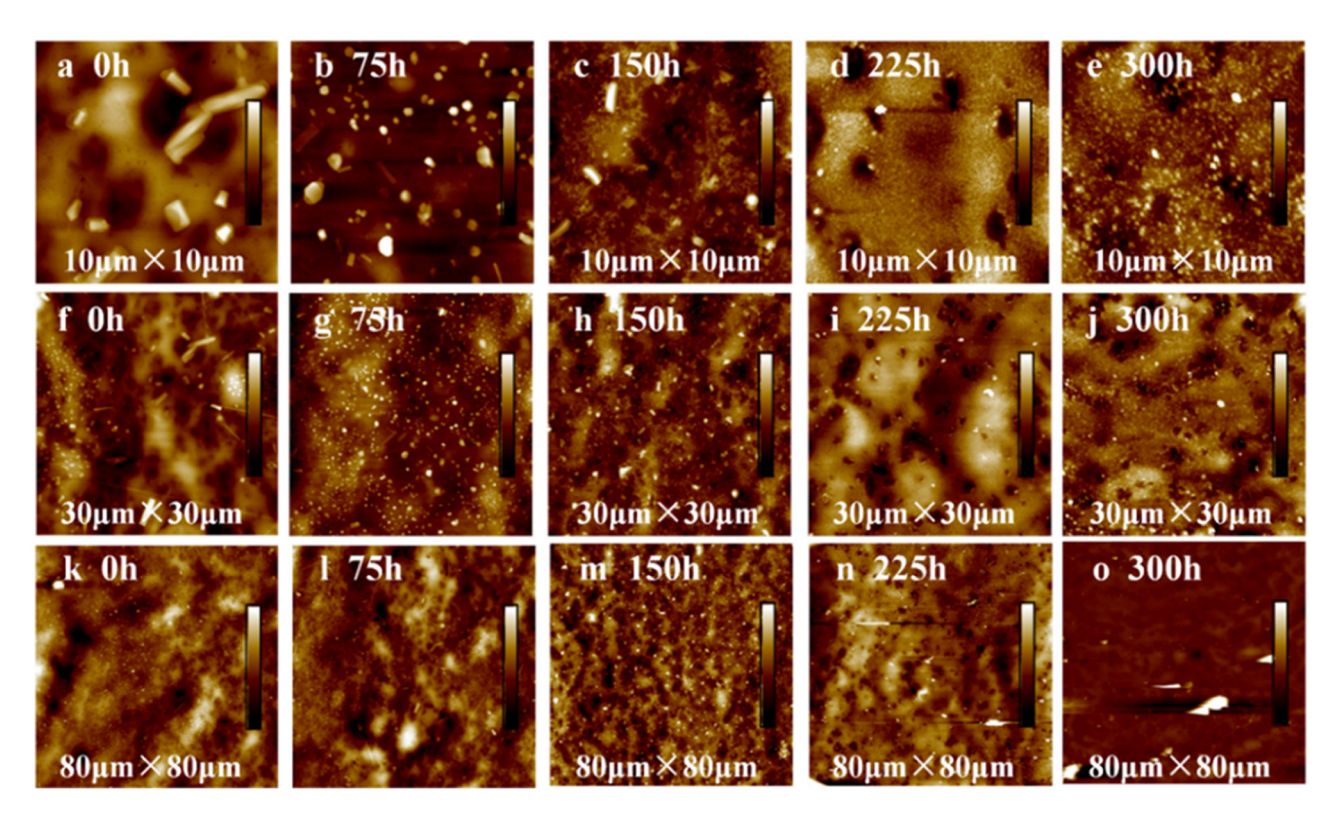


**Figure 15:** Ultraviolet aging surface morphology of AH-70# base asphalt. (a) 0h–10μm, (b) 75h–10μm, (c) 150h–10μm, (d) 225h–10μm, (e) 300h–10μm, (f) 0h–30μm, (g) 75h–30μm, (h) 150h–30μm, (i) 225h–30μm, (j) 300h–30μm, (k) 0h–80μm, (l) 75h–80μm, (m) 150h–80μm, (n) 225h–80μm, and (o) 300h–80μm.

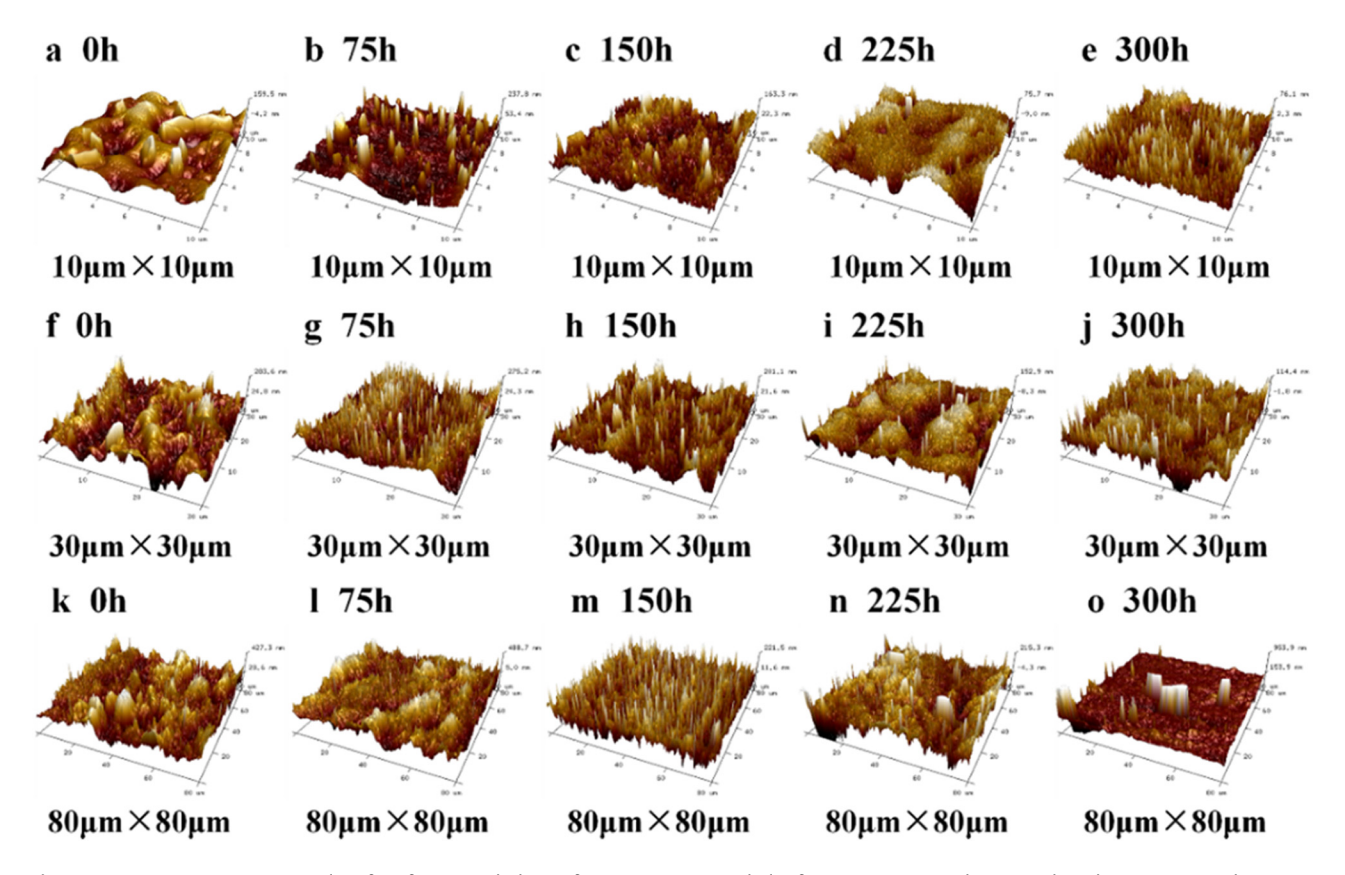


Figure 16: 3D reconstruction results of surface morphology of AH-70# matrix asphalt after UV aging. (a) 0h-10µm, (b) 75h-10µm, (c) 150h-10µm, (d) 225h-10µm, (e) 300h-10µm, (f) 0h-30µm, (g) 75h-30µm, (h) 150h-30µm, (i) 225h-30µm, (j) 300h-30µm, (k) 0h-80µm, (l) 75h-80µm, (m) 150h-80µm, (n) 225h-80µm, and (o) 300h-80µm.

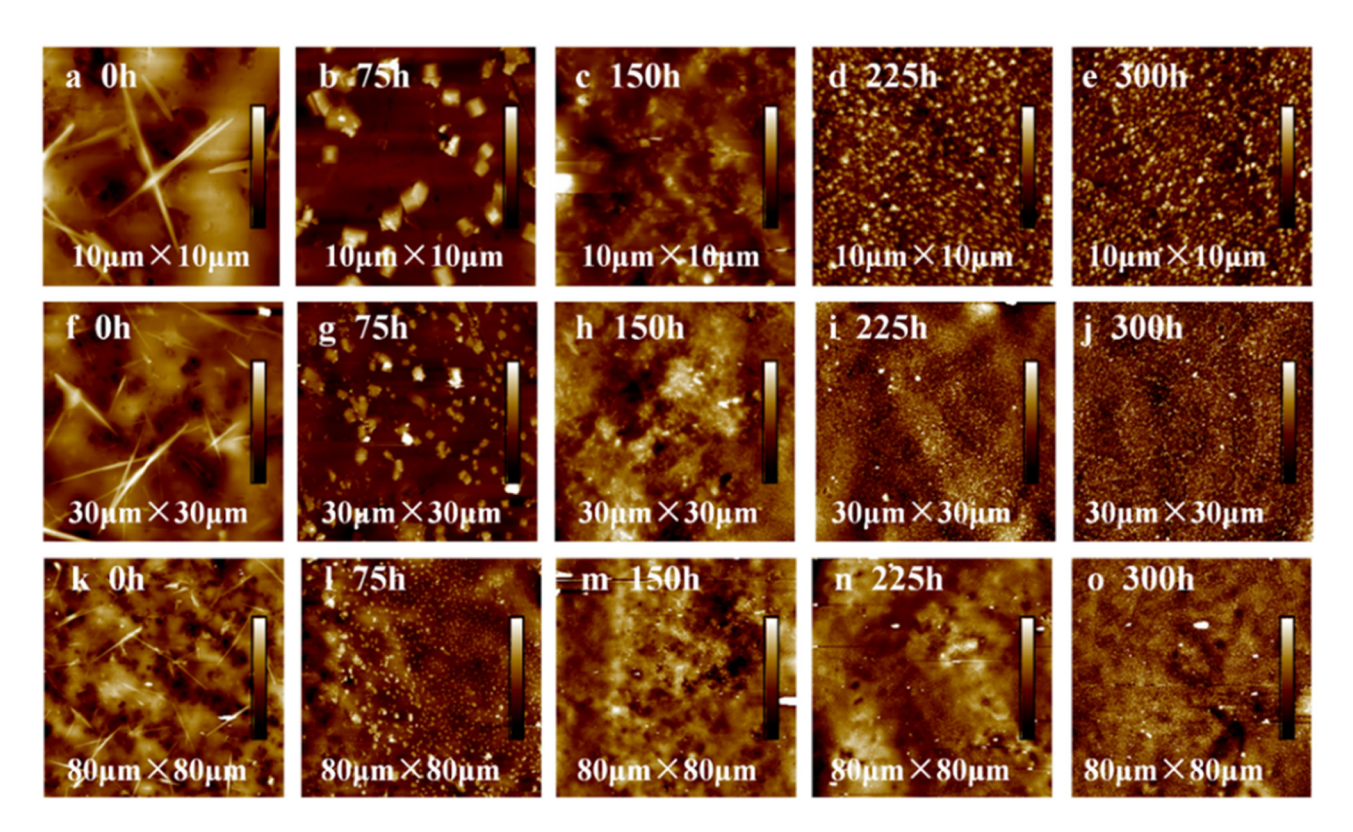
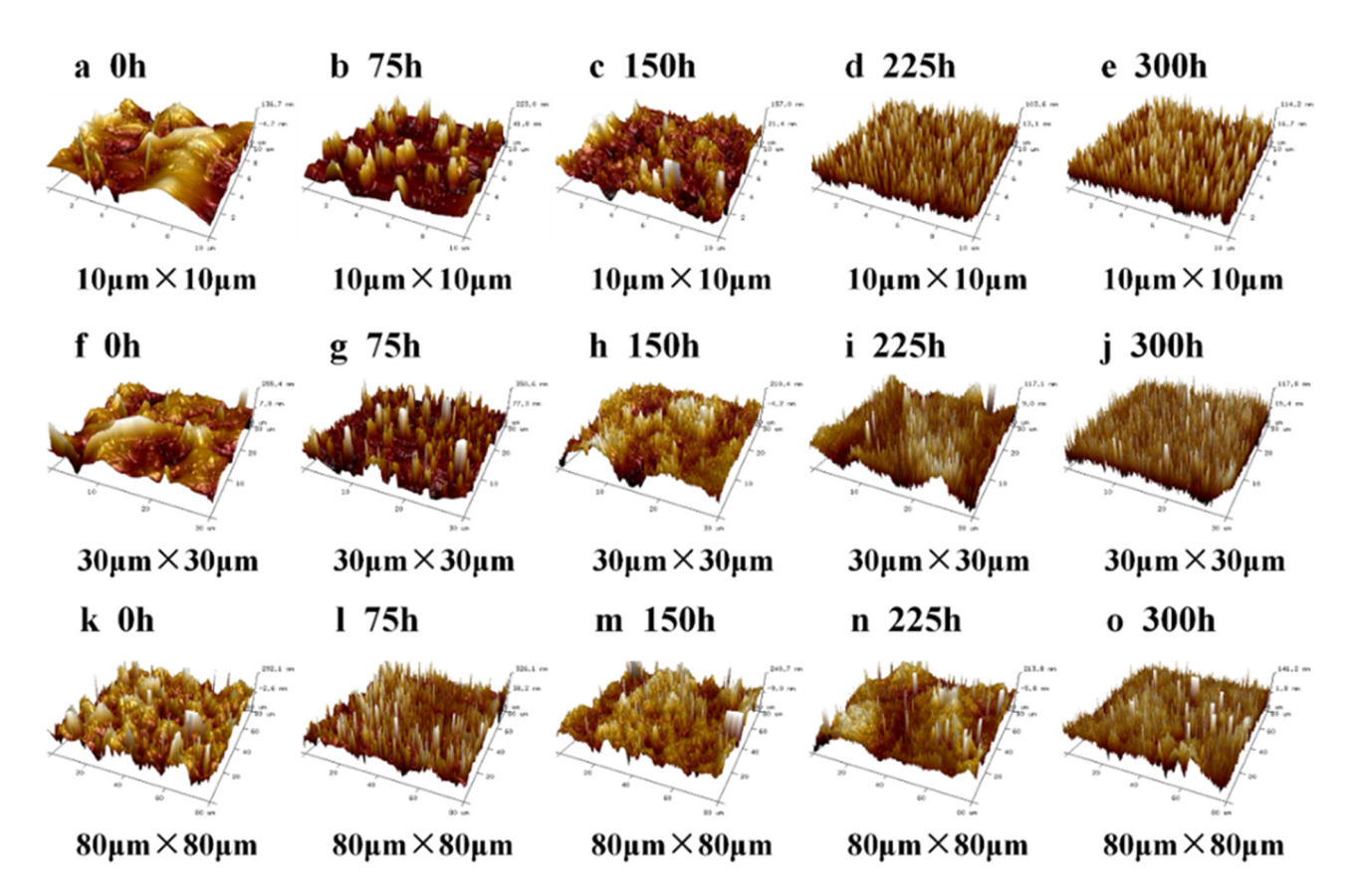


Figure 17: Ultraviolet aging surface morphology of polymer-modified asphalt. (a) 0h-10µm, (b) 75h-10µm, (c) 150h-10µm, (d) 225h-10µm, (e) 300h-10µm, (f) 0h-30µm, (q) 75h-30µm, (h) 150h-30µm, (i) 225h-30µm, (j) 300h-30µm, (k) 0h-80µm, (l) 75h-80µm, (m) 150h-80µm, (n) 225h-80µm, and (o) 300h-80µm.

14 — Honggang Zhang et al. DE GRUYTER



**Figure 18:** 3D reconstruction results of surface morphology of polymer-modified asphalt. (a) 0h–10μm, (b) 75h–10μm, (c) 150h–10μm, (d) 225h–10μm, (e) 300h–10μm, (f) 0h–30μm, (g) 75h–30μm, (h) 150h–30μm, (i) 225h–30μm, (j) 300h–30μm, (k) 0h–80μm, (l) 75h–80μm, (m) 150h–80μm, (n) 225h–80μm, and (o) 300h–80μm.

and 150 h, the surface roughness of PW-modified asphalt increases significantly. However, with the further extension of the UV aging time, the roughness of the asphalt surface decreases significantly, and the density of the independent bulges also increases significantly. The surface roughness of PW-modified asphalt at 225 and 300 h is close to that of PW-modified asphalt, and there is no further improvement. After UV aging for 225 h, the obvious difference in asphalt surface roughness may be caused by the delaying effect of the PW modifier on asphalt UV aging behavior.

# 3.5 Chemical variation of polymer-modified asphalt following UV aging

# 3.5.1 Functional group composition

Figures 19 and 20 show the dynamic FTIR characterization results of base asphalt and PW-modified asphalt. The analysis in Figure 19 shows that the strength of the functional

groups and absorption peaks of the matrix asphalt are basically unchanged during the UV aging process, which indicates that the composition of the functional groups in the asphalt has not changed significantly during the UV aging process. At the same time, during the heating process, the absorption peak of asphalt still appears at the position of 3,000 cm<sup>-1</sup> wave number, and the intensity of the absorption peak also changes to a certain extent, which indicates that different substances will volatilize in the asphalt during the heating process.

According to the analysis in Figure 20, with the change in UV aging time, the dynamic FTIR test results of PW-modified asphalt are different from that of base asphalt. Like the base asphalt, the main absorption peak of PW-modified asphalt also appears at the wave number of 3,000 cm<sup>-1</sup>. However, with the gradual extension of UV aging time, the absorption peak with higher intensity also appeared at 2,400 cm<sup>-1</sup> wave number, which indicates that new functional groups may appear in PW-modified asphalt during UV radiation. This may be directly related to the improvement effect of the PW modifier on asphalt aging resistance.

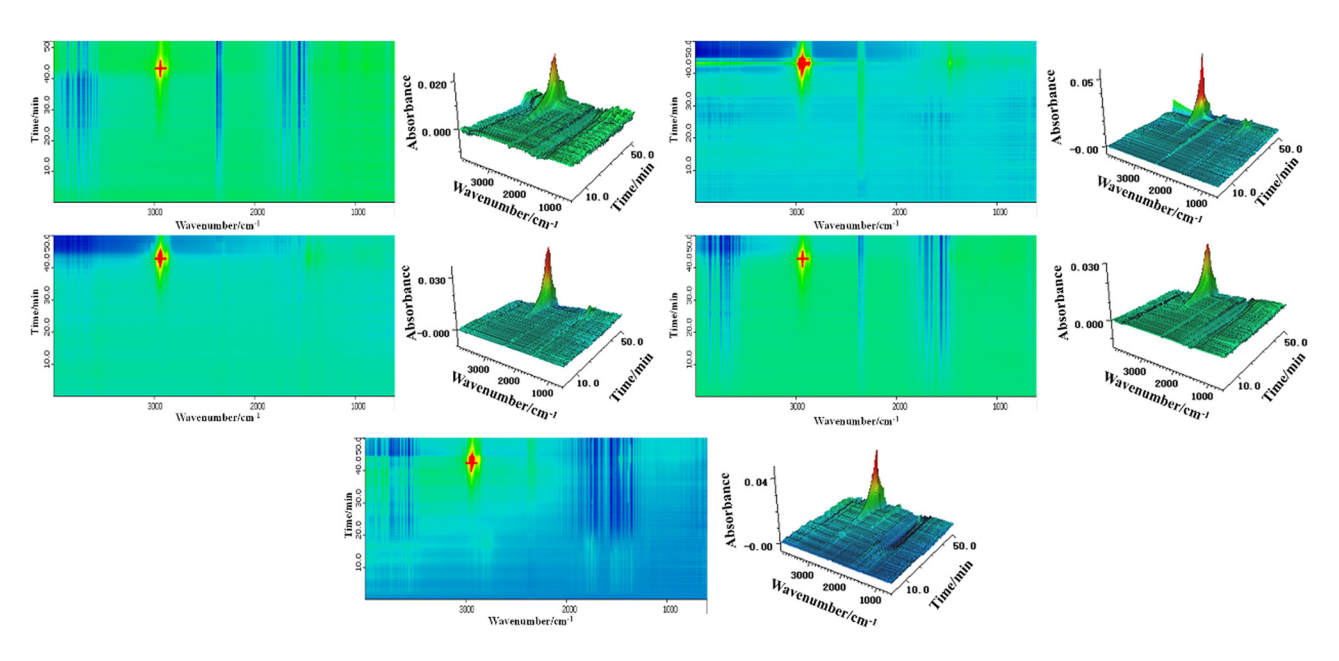


Figure 19: Dynamic FTIR spectrum of AH-70# matrix asphalt under ultraviolet aging.

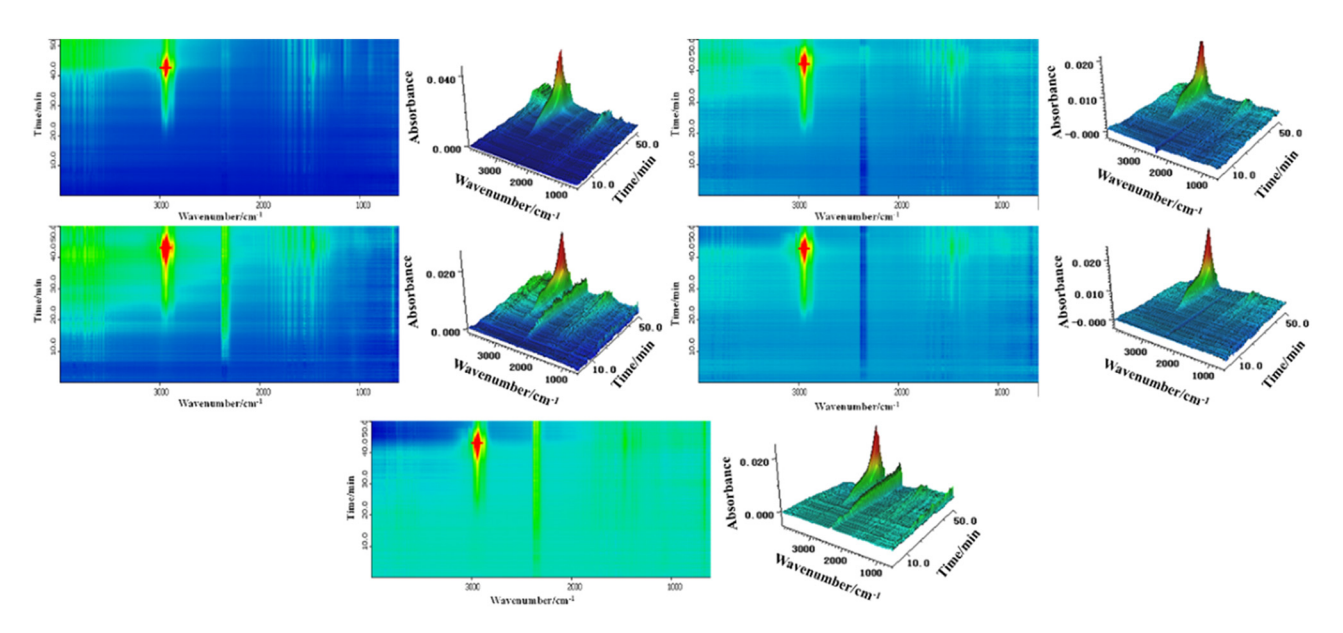
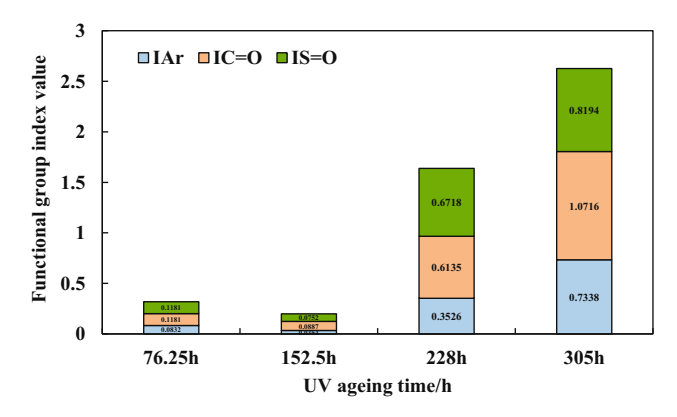


Figure 20: Dynamic FTIR spectrum of polymer-modified asphalt under ultraviolet aging.

# 3.5.2 Functional group indices

Figures 21 and 22 show the functional group index changes of AH-70# matrix asphalt and PW-modified asphalt. According to Figure 21, as the UV aging time prolonged, the aromatic functional groups, carbonyl groups, and sulfoxide group indices in the matrix asphalt increased gradually. When the UV aging time reaches 305 h, the characteristic functional group index reached the maximum value, indicating that the degree of UV aging of the matrix asphalt gradually

became severe with the extension of UV irradiation time, which was basically consistent with the trend of changes in the macroscopic properties. According to Figure 22, it could be analyzed that the characteristic functional group index of PW-modified asphalt first increased and then decreased. When the UV irradiation time exceeded 228 h, the functional group index of carbonyl and sulfoxide groups significantly decreased. Meanwhile, further analysis in Figure 23 shows that the characteristic functional group index of PW-modified asphalt was significantly lower than that of the base asphalt.



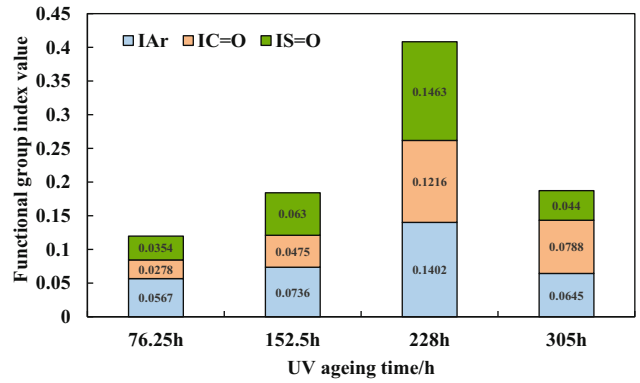


Figure 21: Functional group indices of AH-70# base asphalt.

Figure 22: Functional group indices of PW modified asphalt.

Compared to the matrix asphalt, the characteristic functional group index of PW-modified asphalt decreased by about 18.6 times, indicating that PW modifier could block the formation and accumulation of aging functional groups such as carbonyl and sulfoxide groups inside the asphalt effectively during UV aging, thereby achieving effective control of asphalt UV aging behavior.

# 4 Conclusions

Based on the aforementioned findings, the following conclusions could be drawn:

1) The PW modifier has obvious edges and corners, and the lamellar structure gives the particles a larger specific surface area. The particles are relatively independent,

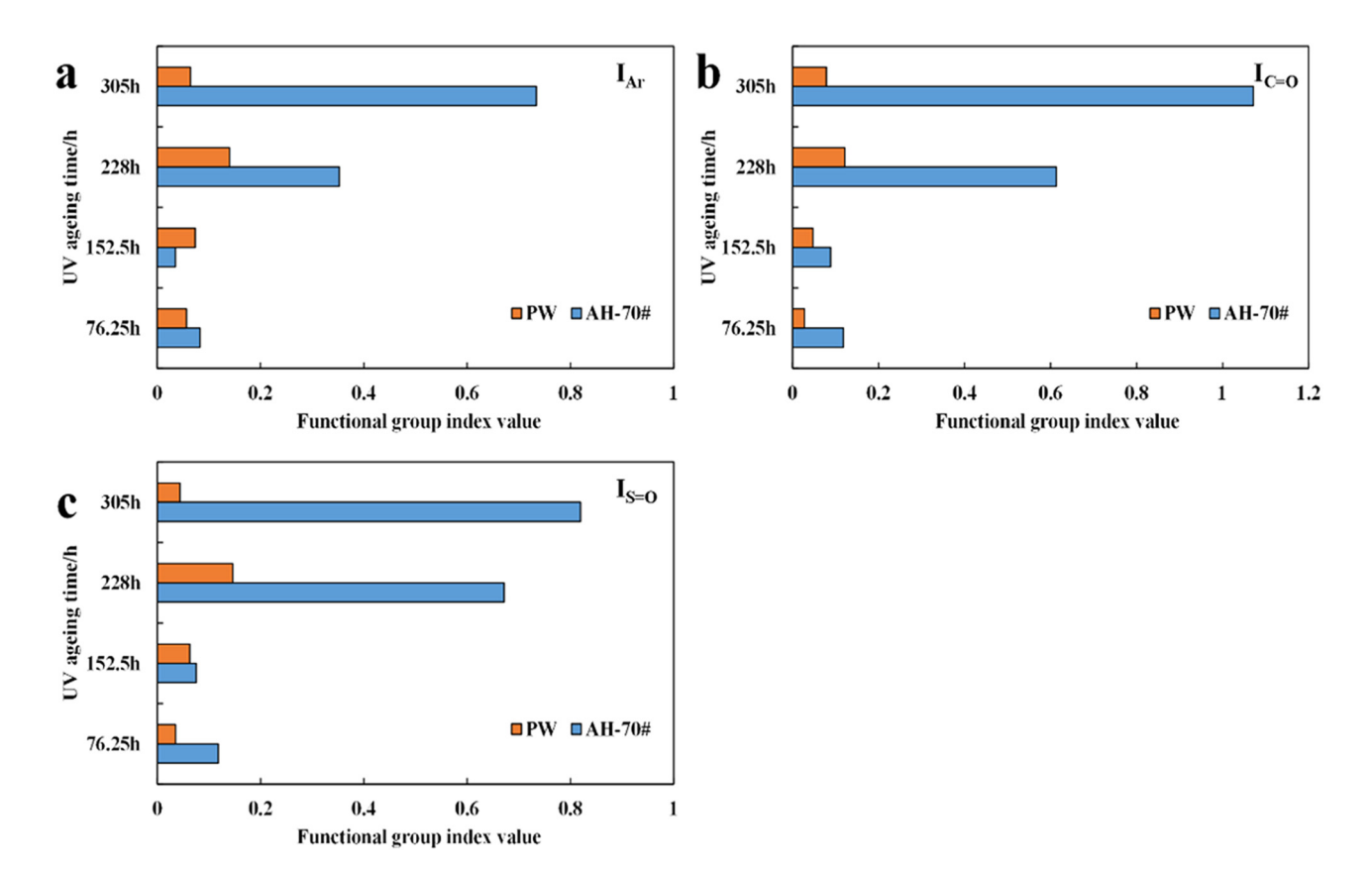


Figure 23: Comparison of functional group indices between PW-modified asphalt and AH-70# asphalt. (a)  $I_{AF}$ , (b)  $I_{C=0}$ , and  $I_{S=0}$ .

- so the PW modifier can form a good bond and interact with asphalt.
- 2) In the infrared spectrum, the accessory shoulder peak appears at 1493.73 cm<sup>-1</sup>, and the benzene ring stretching vibration appears at 1627.12 cm<sup>-1</sup>. The bending vibration of the aromatic ring occurs at 697.23 cm<sup>-1</sup>, while the characteristic peak at about 2,800 cm<sup>-1</sup> is the C-H symmetric stretching of -CH<sub>2</sub>-. With the increase of time, the intensity of each characteristic peak tends to be almost flat at 43 min. There is no obvious change of peak position and the appearance of new groups in the change of temperature.
- 3) The PW modifier has a good control effect on the UV aging of asphalt and can keep the road performance of asphalt after UV aging without significant changes, thus ensuring the stability of service performance.
- 4) With the extension of UV aging time, the number of cracks on the PW-modified asphalt surface decreased significantly, and the width of cracks also decreased significantly. This may be due to the flow and fusion of asphalt, resulting in the partial healing of cracks, thus reducing the number of cracks on the asphalt surface.
- 5) PW modifier could block the formation and accumulation of aging functional groups such as carbonyl and sulfoxide groups inside the asphalt effectively during UV aging, thereby achieving effective control of asphalt UV aging behavior.

Acknowledgments: This article describes research activities mainly supported by Guangxi Key Lab of Road structure and materials (2021gxjgclkf003), supported by the Fundamental Research Funds for the Central Universities under grant number 300102212516, supported by the open research fund of Highway Engineering Key Laboratory of Sichuan Province, Southwest Jiaotong University (HEKLSP2022-8). That sponsorship and interest are gratefully acknowledged.

Funding information: Guangxi Key Lab of Road structure and materials (2021gxjgclkf003), Fundamental Research Funds for the Central Universities (300102212516), Open research fund of Highway Engineering Key Laboratory of Sichuan Province, Southwest Jiaotong University (HEKLSP2022-8), and Special Fund for Science and Technology Innovation Strategy of Guangdong Province (pdjh2022b0161).

**Authors contributions:** All authors contributed to the study conception and design. Material preparation, data collection, and analysis were performed by Honggang Zhang, Weian Xuan, Xiaolong Sun, Jie Chen, and Yunchu Zhu. The first draft of the manuscript was written by Xiaolong Sun

and Yunchu Zhu, and all authors commented on previous versions of the manuscript. All authors have accepted responsibility for the entire content of this manuscript and approved its submission.

**Conflict of interest:** The authors state no conflict of interest.

Data availability statement: The datasets generated and/ or analysed during the current study are available from the corresponding author on reasonable request.

# References

- Zhang, H. and D. Zhang. Effect of different inorganic nanoparticles on physical and ultraviolet aging properties of bitumen. Journal of Materials in Civil Engineering, Vol. 27, No. 12, 2015, id. 04015049.
- Wang, C., Y. Li, P. Wen, W. Zeng, and X. Wang. A comprehensive [2] review on mechanical properties of green controlled low strength materials. Construction and Building Materials, Vol. 63, 2023, id. 129611.
- Yu, H., Z. Zhu, Z. Leng, C. Wu, Z. Zhang, D. Wang, et al. Effect of mixing sequence on asphalt mixtures containing waste tire rubber and warm mix surfactants. Journal of Cleaner Production, Vol. 246, 2020, id. 119008.
- Jin, J., Y. Gao, Y. Wu, S. Liu, R. Liu, H. Wei, et al. Rheological and [4] adhesion properties of nano-organic palygorskite and linear SBS on the composite modified asphalt. Powder Technology, Vol. 377, 2021, pp. 212-221.
- Yu, H., D. Yao, G. Qian, J. Cai, X. Gong, and L. Cheng. Effect of ultraviolet aging on dynamic mechanical properties of SBS modified asphalt mortar. Construction and Building Materials, Vol. 281, 2021, id. 122328.
- Zhang, H., Z. Chen, G. Xu, and C. Shi. Evaluation of aging behaviors of asphalt binders through different rheological indices. Fuel, Vol. 221, 2018, pp. 78-88.
- Sun, X., Z. Ou, Q. Xu, X. Qin, Y. Guo, J. Lin, et al. Feasibility analysis of resource application of waste incineration fly ash in bitumen pavement materials. Environmental Science and Pollution Research, Vol. 30, No. 2, 2023, pp. 5242-5257.
- Yu, H., G. Deng, Z. Zhang, M. Zhu, M. Gong, and M. Oeser. Workability of rubberized asphalt from a perspective of particle effect. Transportation Research Part D: Transport and Environment, Vol. 91, 2021, id. 102712.
- [9] Sun, X., Y. Zhang, Q. Peng, J. Yuan, Z. Cang, and J. Lv. Study on adaptability of rheological index of nano-PUA-modified asphalt based on geometric parameters of parallel plate. Nanotechnology Reviews, Vol. 10, No. 1, 2021, pp. 1801-1811.
- Zhang, H., J. Yu, H. Wang, and L. Xue. Investigation of microstructures and ultraviolet aging properties of organo-montmorillonite/ SBS modified bitumen. Materials Chemistry and Physics, Vol. 129, No. 3, 2011, pp. 769-776.
- [11] Yu, H., X. Bai, G. Qian, H. Wei, X. Gong, J. Jin, et al. Impact of ultraviolet radiation on the aging properties of SBS-modified bitumen binders. Polymers, Vol. 11, No. 7, 2019, id. 1111.
- **[121** Sun, X., Q. Peng, Y. Zhu, Q. Chen, J. Yuan, and Y. Zhu. Effects of UV Aging on Physical Properties and Physicochemical Properties of

- ASA Polymer-Modified Asphalt. *Advances in Materials Science and Engineering*, Vol. 2022, No. 1, 2022, id. 1157687.
- [13] Sun, X., Q. Peng, Y. Zhu, J. Jin, J. Xu, Y. Yin, et al. Modification and enhancing effect of SPUA material on bitumen binder: A study of viscoelastic properties and microstructure characterization. *Case Studies in Construction Materials*, Vol. 18, 2023, id. e01781.
- [14] Qin, X. and X. Sun. Quantitative investigation and decision support of reducing effect of warm mixed bitumen mixture (WMA) on emission and energy consumption in highway construction. *Environmental Science and Pollution Research*, Vol. 29, No. 22, 2022, pp. 33383–33399.
- [15] Liu, Z., X. Sun, X. Qin, and Y. Yin. Micro-analysis of the fusion process between light stabilizer and asphalt using different characterizing methods. *Construction and Building Materials*, Vol. 287, 2021. id. 123045.
- [16] Yang, X., H. Tang, X. Cai, K. Wu, W. Huang, Q. Zhang, et al. Evaluating reclaimed asphalt mixture homogeneity using force chain transferring stress efficiency. *Construction and Building Materials*, Vol. 365, 2023, id. 130050.
- [17] Sun, X., Q. Xu, G. Fang, Y. Zhu, Z. Yuan, Q. Chen, et al. Effect Investigation of Ultraviolet Ageing on the Rheological Properties, Micro-Structure, and Chemical Composition of Asphalt Binder Modified by Modifying Polymer. Advances in Materials Science and Engineering, Vol. 2022, No. 1, 2022, id. 7190428.
- [18] Li, Y., J. Feng, S. Wu, A. Chen, D. Kuang, Y. Gao, et al. Review of ultraviolet ageing mechanisms and anti-ageing methods for asphalt binders. *Journal of Road Engineering*, Vol. 2, No. 2, 2022, pp. 137–155.
- [19] Yang, B., H. Li, Y. Sun, H. Zhang, J. Liu, J. Yang, et al. Chemo-rheo-logical, mechanical, morphology evolution and environmental impact of aged asphalt binder coupling thermal oxidation, ultraviolet radiation and water. *Journal of Cleaner Production*, No. 388, 2023, id. 135866.
- [20] Sun, X., X. Qin, Z. Liu, Y. Yin, C. Zou, and S. Jiang. New preparation method of bitumen samples for UV aging behavior investigation. *Construction and Building Materials*, Vol. 233, 2020, id. 117278.

- [21] Zhang, H., H. Duan, C. Zhu, Z. Chen, and H. Luo. Mini-review on the application of nanomaterials in improving anti-aging properties of asphalt. *Energy & Fuels*, Vol. 35, No. 14, 2021, pp. 11017–11036.
- [22] Jin, J., Y. Gao, Y. Wu, R. Li, R. Liu, H. Wei, et al. Performance evaluation of surface-organic grafting on the palygorskite nanofiber for the modification of asphalt. *Construction and Building Materials*, Vol. 268, 2021, id. 121072.
- [23] Chen, Q., C. Wang, Y. Li, L. Feng, and S. Huang. Performance development of polyurethane elastomer composites in different construction and curing environments. *Construction and Building Materials*, Vol. 365, 2023, id. 130047.
- [24] Guo, M., M. Liang, A. Sreeram, A. Bhasin, and D. Luo. Characterization of rejuvenation of various modified asphalt binders based on simplified chromatographic techniques. *International Journal of Pavement Engineering*, Vol. 23, No. 12, 2022, pp. 4333–4343.
- [25] Pei, Z., M. Xu, J. Cao, D. Feng, W. Hu, J. Ren, et al. Analysis of the micro characteristics of different kinds of asphalt based on different aging conditions. *Materials and Structures*, Vol. 55, No. 10, 2022, pp. 1–18.
- [26] Zhu, C., H. Zhang, D. Zhang, and Z. Chen. Influence of base asphalt and SBS modifier on the weathering aging behaviors of SBS modified asphalt. *Journal of Materials in Civil Engineering*, Vol. 30, No. 3, 2018, id. 04017306.
- [27] Gao, M., C. Fan, X. Chen, and M. Li. Study on ultraviolet aging performance of composite modified asphalt based on rheological properties and molecular dynamics simulation. *Advances in Materials Science and Engineering*, Vol. 2022, No. 1, 2022, id. 7894190.
- [28] Song, S., M. Liang, L. Wang, D. Li, M. Guo, L. Yan, et al. Effects of different natural factors on rheological properties of sbs modified asphalt. *Materials*, Vol. 15, No. 16, 2022, id. 5628.
- [29] Yang, S., K. Yan, and W. Liu. The effect of ultraviolet aging duration on the rheological properties of sasobit/SBS/nano-TiO<sub>2</sub>modified asphalt binder. *Applied Sciences*, Vol. 12, No. 20, 2022, id. 10600.